

Entanglement generation and measurement in electron quantum optics

M2 internship (13/01/2025 - 04/07/2025)

Mathieu Paulet - École Centrale de Lyon, Lyon - July 8th, 2025



Summary

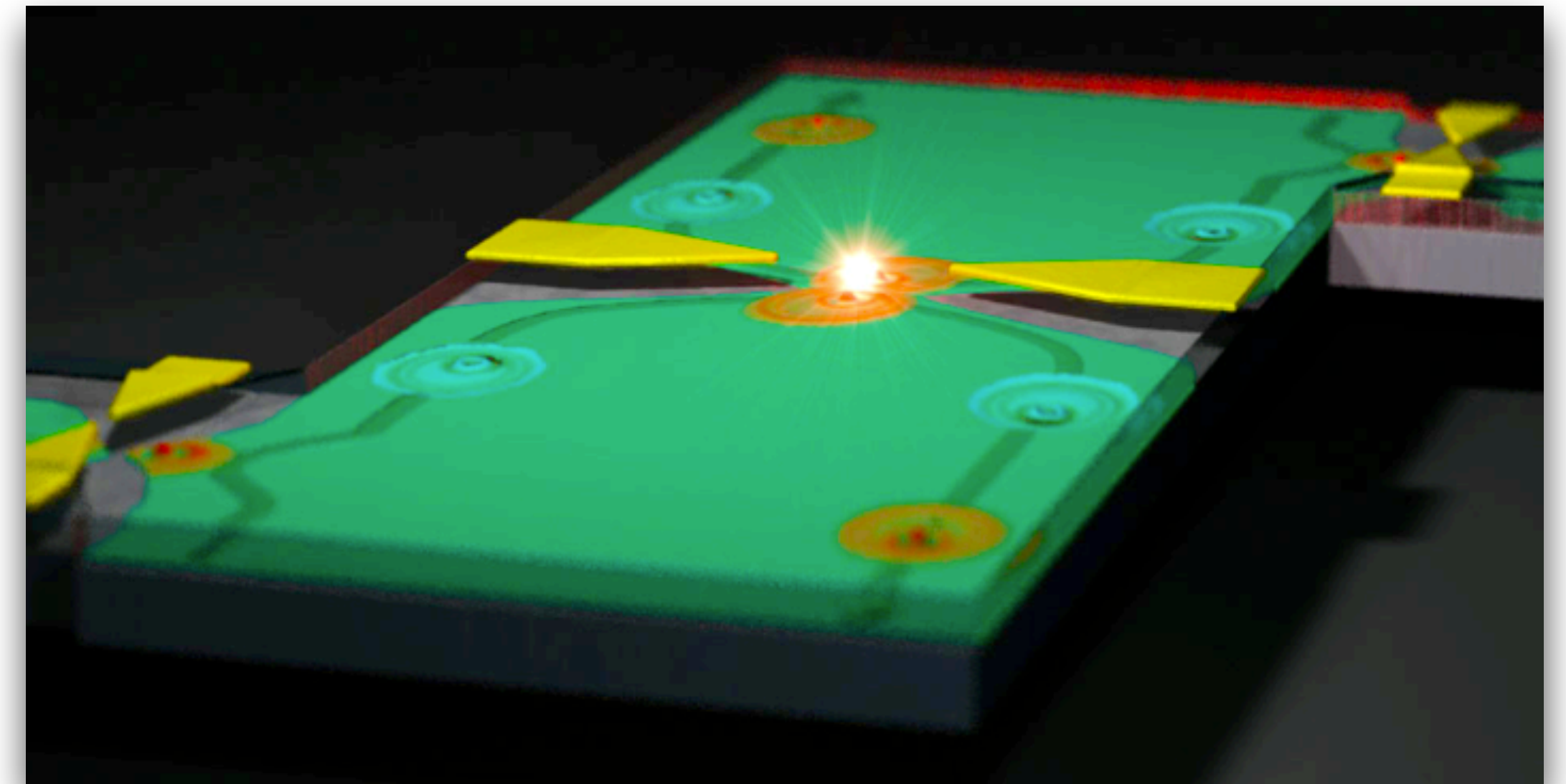
Introduction and context

I. Electron quantum optics

II. Quantum tomography protocols

III. Two-electron coherent scattering

Conclusion and perspectives



Marguerite et al., Physica status solidi (b) 254, 3 (Dec. 2016).

Introduction and context

Introduction and context

- **Electron quantum optics:** single electrons in **coherent** quantum conductors
- **Quantum computing:** encoding **quantum information** into electronic states
 - Performing operations on **propagating** electrons: **electronic flying qubits**
 - **Coulomb interaction:** facilitates operations with **several e-qubits**
- (1) **Efficiently** determinate electronic quantum states: **quantum tomography**
- (2) Understand the **collision-induced entanglement:** **entanglement witness** and **two-electron scattering**

I. Electron quantum optics

Differences between EQO and PQO

General definitions and comparisons

Definitions

- **Boson:** particle with an integer spin
- **Fermion:** particle with a half-integer spin
- **Fermi sea:** energy levels filled by the electrons of a system at equilibrium
- **Fermi energy:** energy of the Fermi sea's highest filled level
- **Reference state:** equilibrium state of a system, on top of which any excitation is created

	PQO	EQO
Particle	Photon (<i>spin 1</i>)	Electron (<i>spin 1/2</i>)
Statistics	Bose-Einstein (<i>symmetric</i>)	Fermi-Dirac (<i>anti-symmetric</i>)
Reference state	Vacuum (<i>0 photon</i>)	Fermi sea (<i>many electrons</i>)
Interaction	None	Coulomb repulsion

First-order electronic coherence

Definition and properties

- **First-order coherence function:** $\mathcal{G}_{\hat{\rho}}^{(e)}(t; t') := \langle \hat{\psi}^\dagger[t'] \hat{\psi}[t] \rangle_{\hat{\rho}} = \text{Tr}(\hat{\rho} \hat{\psi}^\dagger[t'] \hat{\psi}[t])$
 - **One-electron physics** in a quantum conductor: overlap between **detection events** at t and t'
 - **Excess of coherence** compared to the coherence of the Fermi sea: $\mathcal{G}_{\hat{\rho}}^{(e)} := \mathcal{G}_F^{(e)} + \Delta \mathcal{G}_{\hat{\rho}}^{(e)}$
- Experimentally linked to the **average current**: $\langle i(t) \rangle_{\hat{\rho}} = -ev_F \Delta \mathcal{G}_{\hat{\rho}}^{(e)}(t; t)$
- **Wigner representation:** $\mathcal{W}_{\hat{\rho}}^{(e)}(t; \omega) := v_F \int_{\mathbb{R}} dt' \mathcal{G}_{\hat{\rho}}^{(e)}(t; t') e^{i\omega t'}$

Second-order electronic coherence

Definition and properties

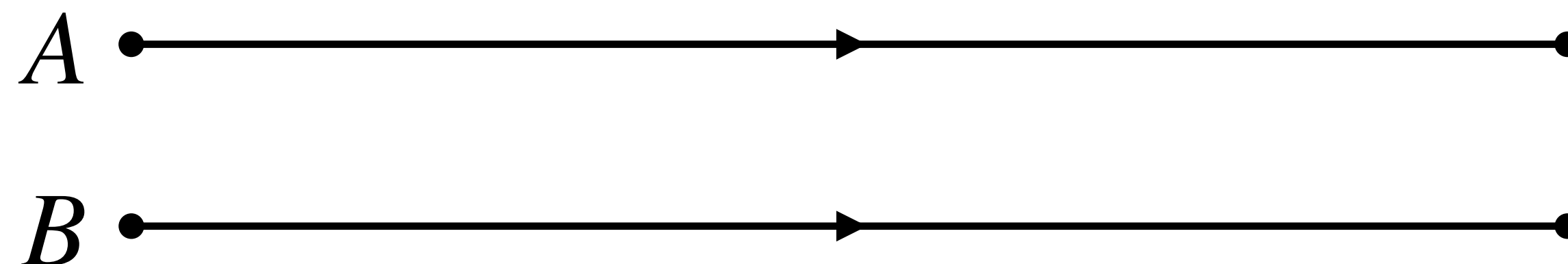
- **Second-order coherence function:** $\mathcal{G}_{\hat{\rho}}^{(2e)}(t_1, t_2; t'_1, t'_2) := \langle \hat{\psi}^\dagger[t'_1] \hat{\psi}^\dagger[t'_2] \hat{\psi}[t_2] \hat{\psi}[t_1] \rangle_{\hat{\rho}}$
 - **Two-electron physics:** overlap between **detection events** at (t_1, t_2) and (t'_1, t'_2)
 - **Excess of coherence:** $\mathcal{G}_{\hat{\rho}}^{(2e)} := \mathcal{G}_F^{(2e)} + \left(\Delta \mathcal{G}_{\hat{\rho}}^{(e)} \mathcal{G}_F^{(e)} + \mathcal{G}_F^{(e)} \Delta \mathcal{G}_{\hat{\rho}}^{(e)} \right) - (\leftrightarrow) + \Delta \mathcal{G}_{\hat{\rho}}^{(2e)}$
- Associated **Wigner representation:**

$$\mathcal{W}_{\hat{\rho}}^{(2e)}(t_1, \omega_1; t_2, \omega_2) := v_F^2 \iint_{\mathbb{R}^2} dt'_1 dt'_2 \mathcal{G}_{\hat{\rho}}^{(2e)}(t_1, t_2; t'_1, t'_2) e^{i(\omega_1 t'_1 + \omega_2 t'_2)}$$

Railroad qubit

Fermionic qubit architecture

- Two parallel **chiral** propagation channels: **quantum Hall edge channels**
- **Qubit architecture** imposed by the **parity super-selection rule (PSSR)**
 - **No superposition** of fermionic states with number of particles of **different parities**
 - Delocalization of **one excitation** on both channels: **respects the PSSR**
- **More stable** than « usual » qubits as 0 and 1 states have **the same energy**

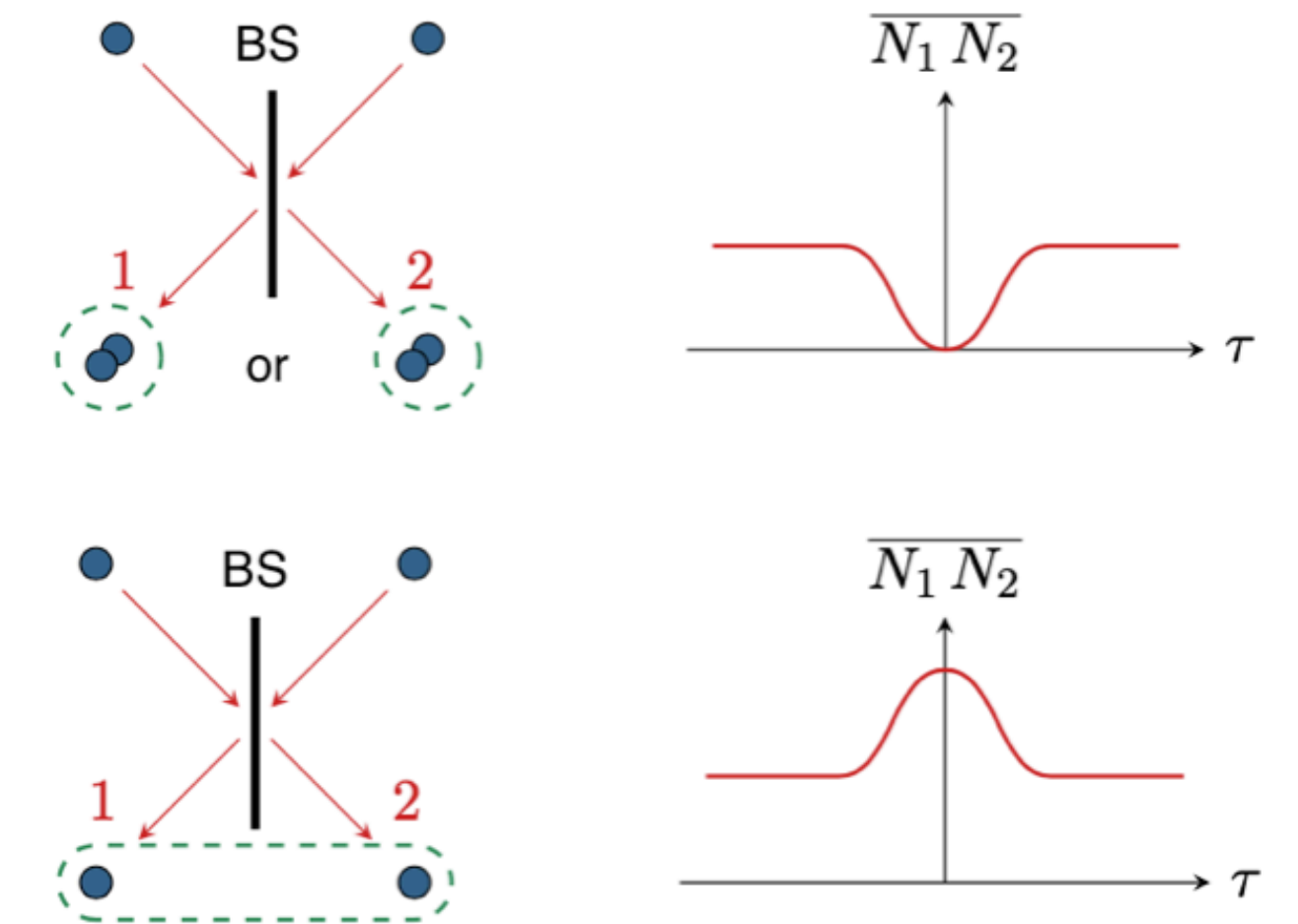
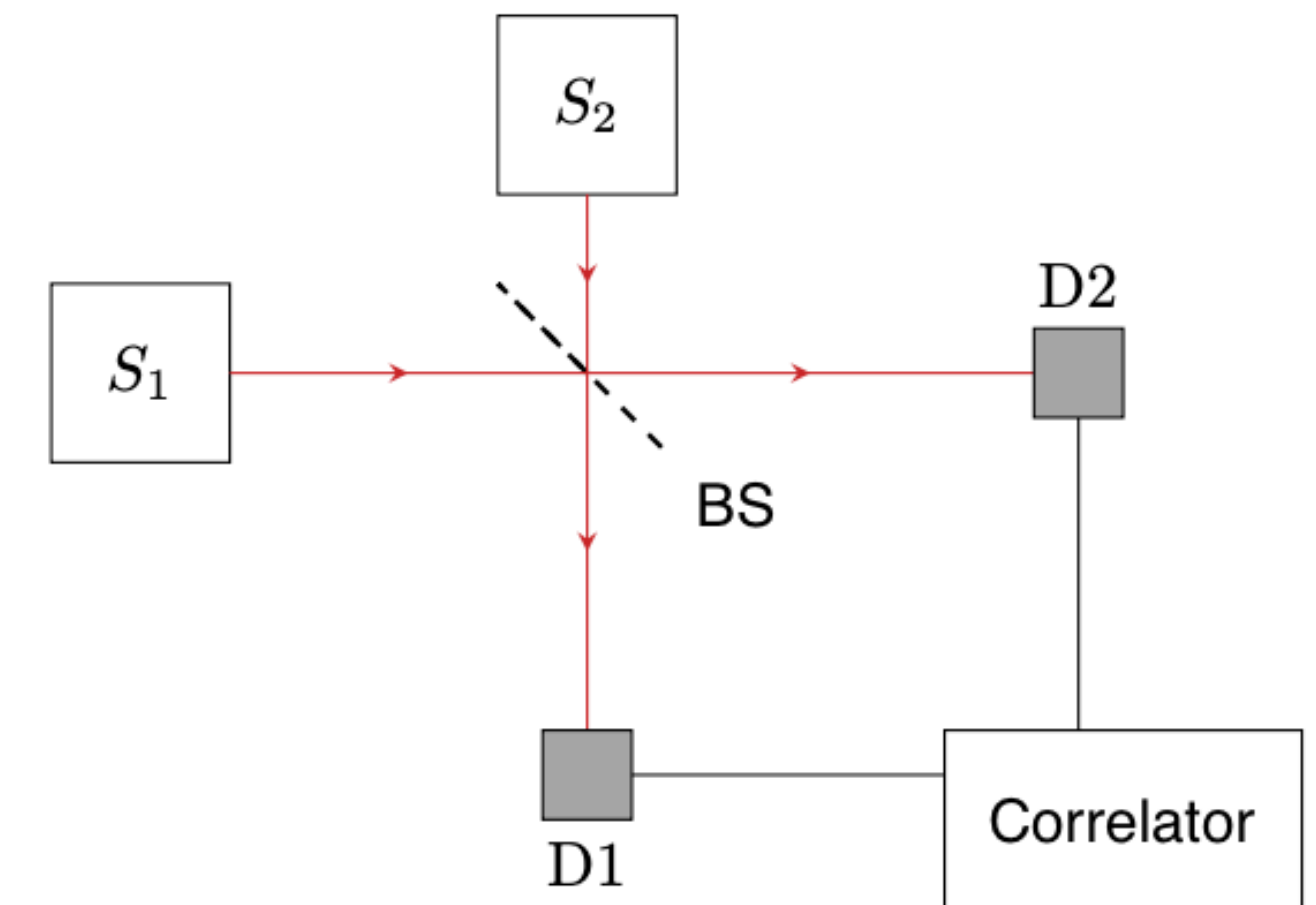


II. Quantum tomography protocols

Hong-Ou-Mandel interferometry

Principle of the experimental setup

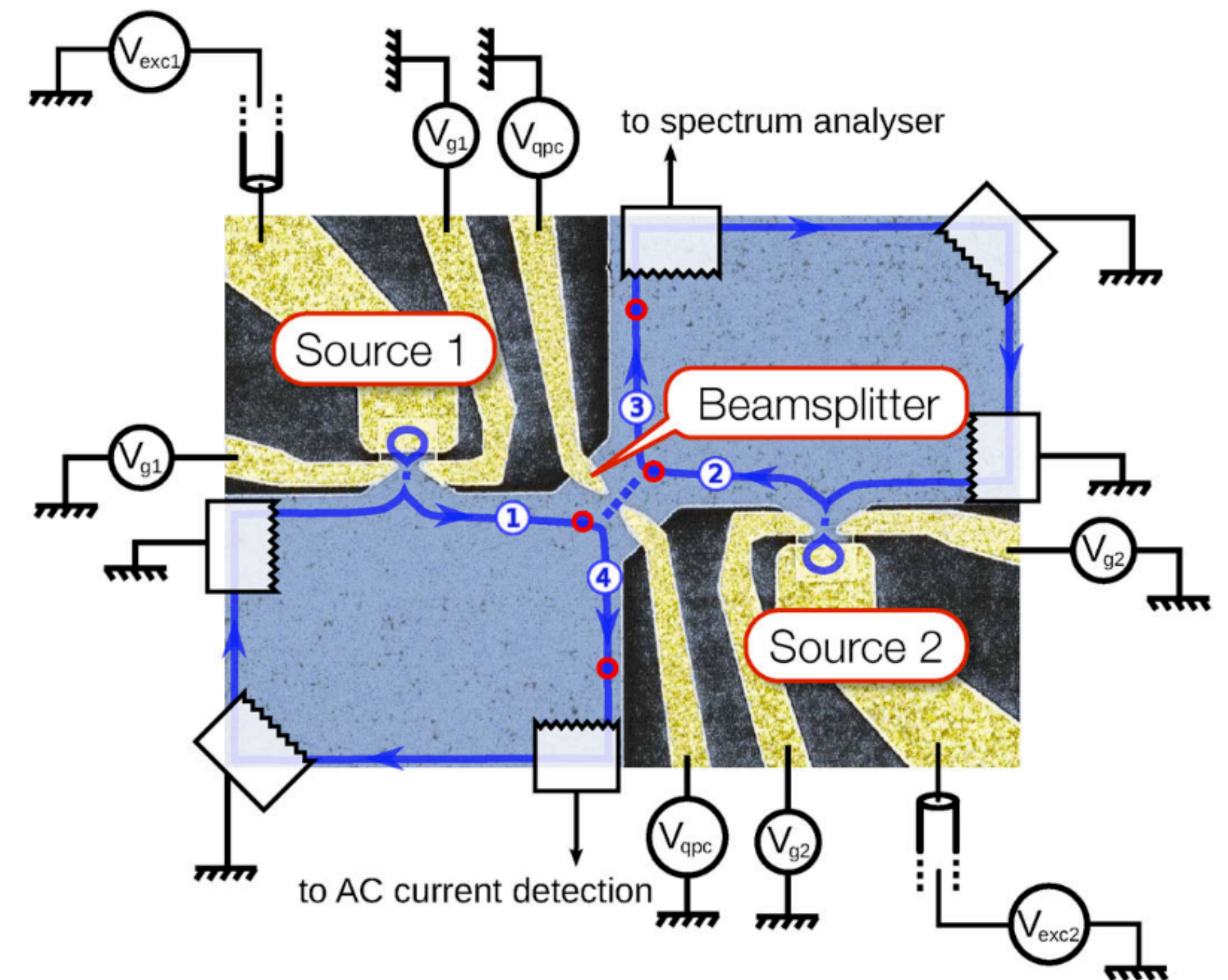
- HOM experiment: **two-particle** interferometry
 - Sending two photons on a **beam-splitter**
 - **Dip in the number correlations** after the beam splitter when two photons income **simultaneously**
- **Bosons** exit the beam-splitter **in the same channel**
- **Fermions** tend to exit **in two different channels**
 - Consequence of **Pauli's exclusion principle**



Hong-Ou-Mandel interferometry

Quantum tomography protocol

- **Electronic** HOM interferometer
 - **Unknown** and **probe** electrons incoming in channels **1** and **2**
 - Unknown excitation probed by a **set of sinusoidal probe signals** $V_{P_n}(t) = V_{DC} + V_{P_n} \cos(2i\pi nft)$
- **Noise in current** measured after interaction
- Overlap between the two incoming **first-order coherences**

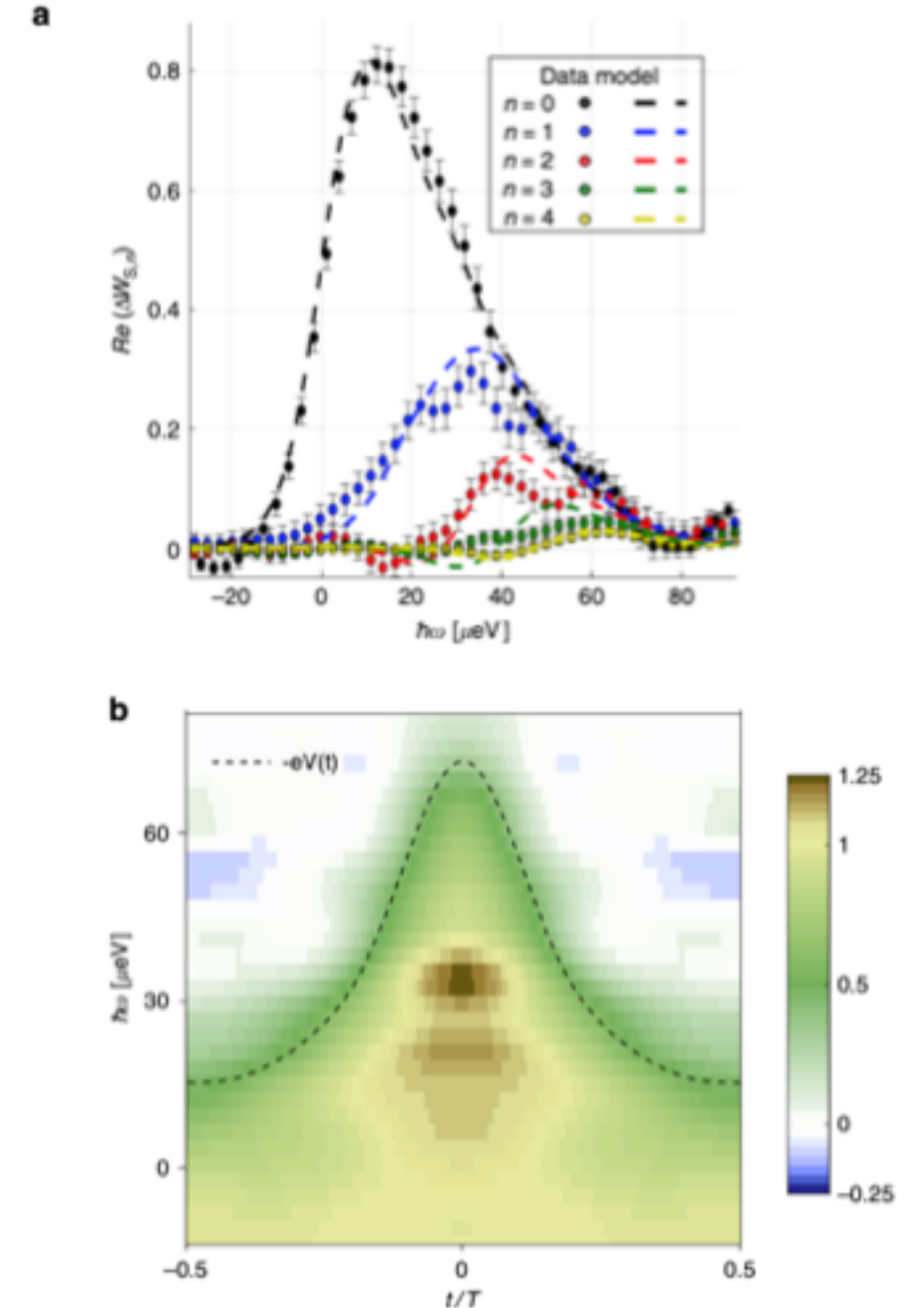


Marguerite et al., Physica status solidi (b) 254, 3 (Dec. 2016).

Hong-Ou-Mandel tomography

Example and limitations

- **Lorentzian** « unknown » excitation
 - **Excellent agreement** with theory for the five first harmonics of $\Delta\mathcal{W}$
 - Precise determination of the **electron's wave-function**
- **One important limitation**
 - May require a **large number of harmonics**
 - **Important amount of time** for a single wave-function (~ 2 days of **non-stop** measurements)

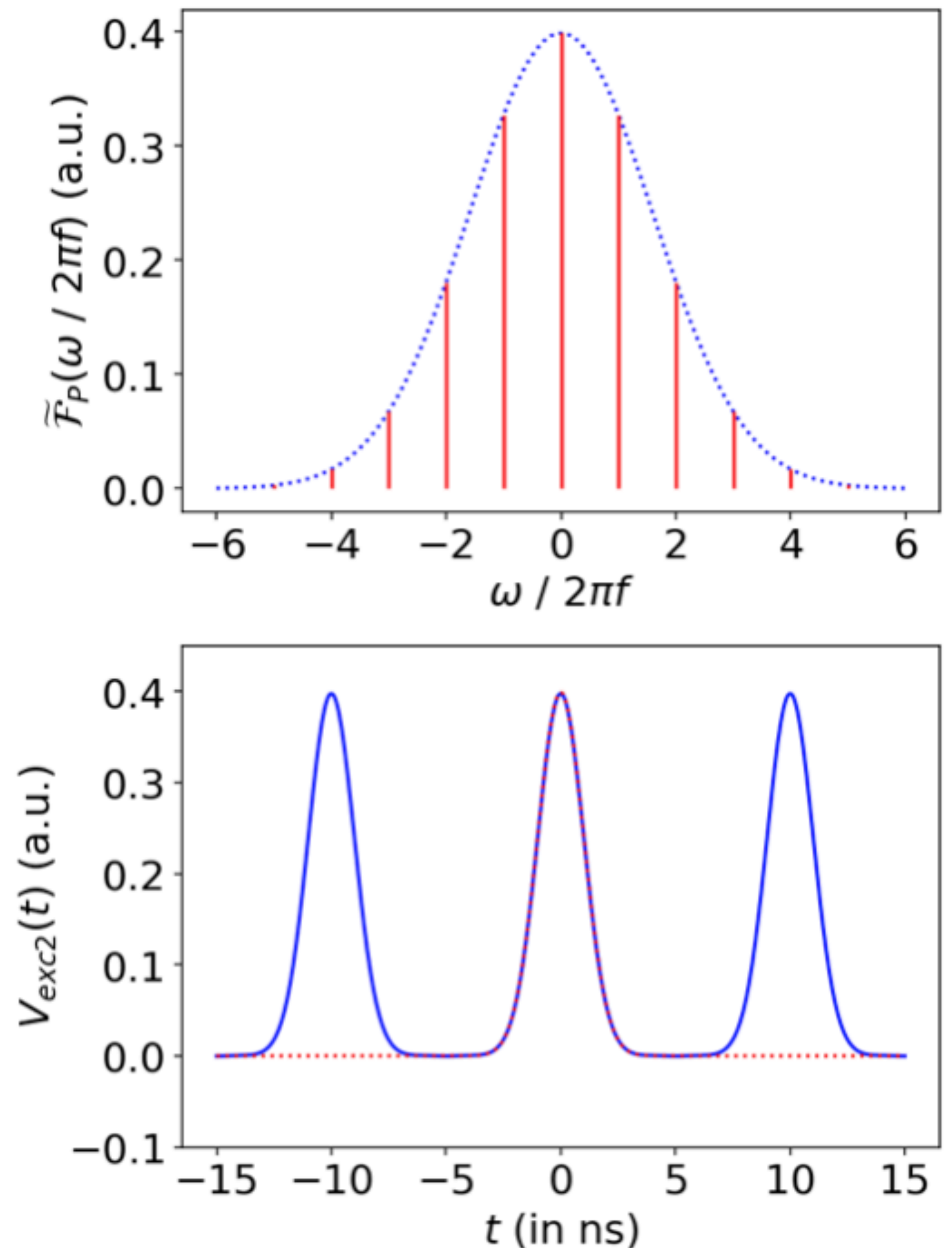


Voltage pulse-train tomography

Principle and illustration

- Determinate the coherence with **linear combinations of sinusoidal signals** ($q_P = e \ll 1$)
 - Probe signals: **voltage pulse-trains** of wavelets \mathcal{F}
 - More suitable to precisely **probe the coherence space**
- Example: **excellent reproduction** of a Gaussian wavelet with only $N = 5$ harmonics

$$\mathcal{F}_P(t) = \frac{1}{\sqrt{2\pi}} \exp\left(-\frac{1}{2}\left(\frac{t}{\tau_0}\right)^2\right)$$

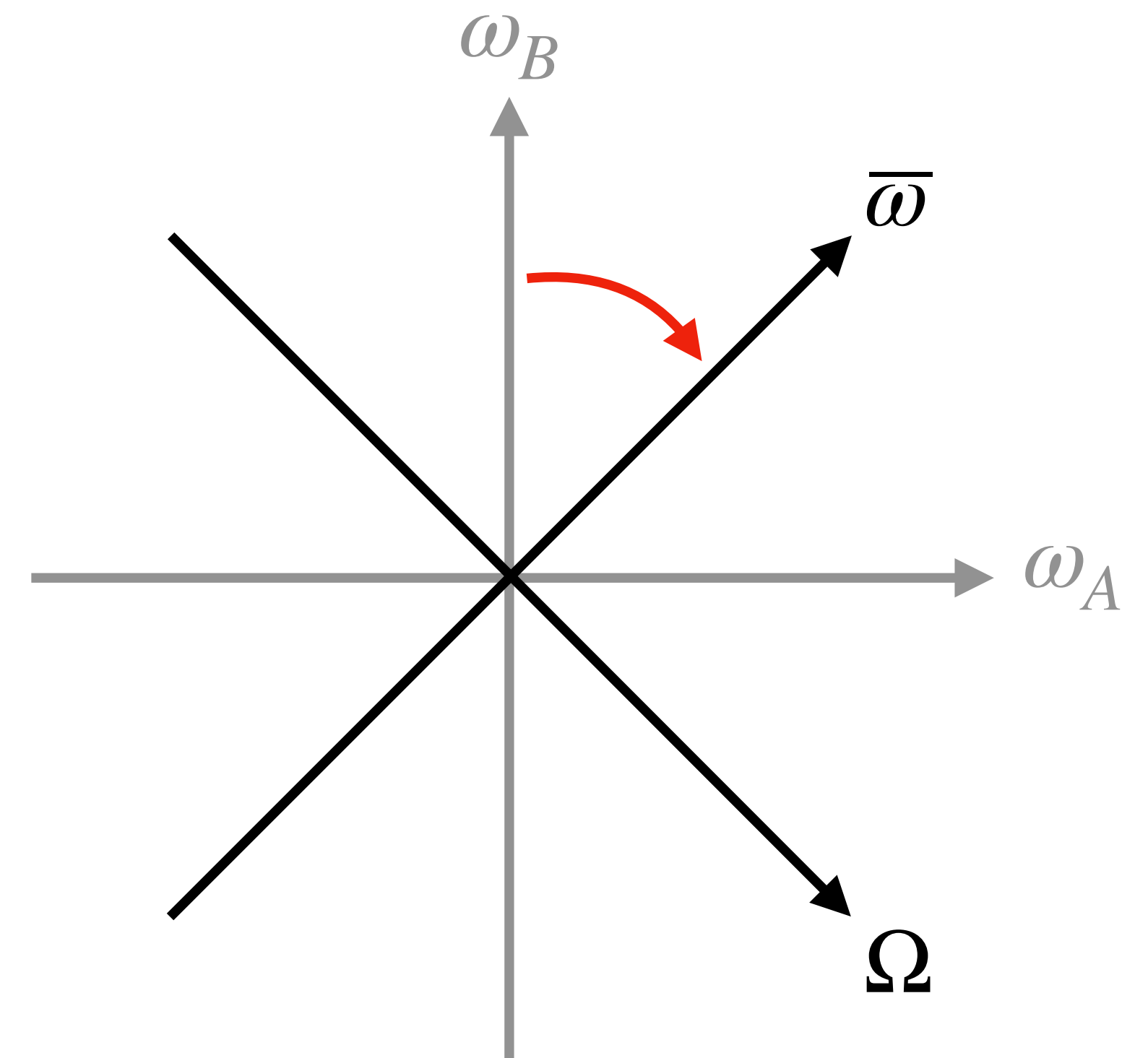


First-order coherence function

Frequency space representation

- **First-order coherence** $\widetilde{\mathcal{G}}_{\hat{\rho}}^{(e)}(\omega_A; \omega_B)$
 - Change of variables: $(\bar{\omega}, \Omega) = \left(\frac{\omega_A + \omega_B}{2}, \omega_A - \omega_B \right)$
 - **Average energy $\bar{\omega}$: diagonal component**
 - Energy **difference Ω : off-diagonal component**

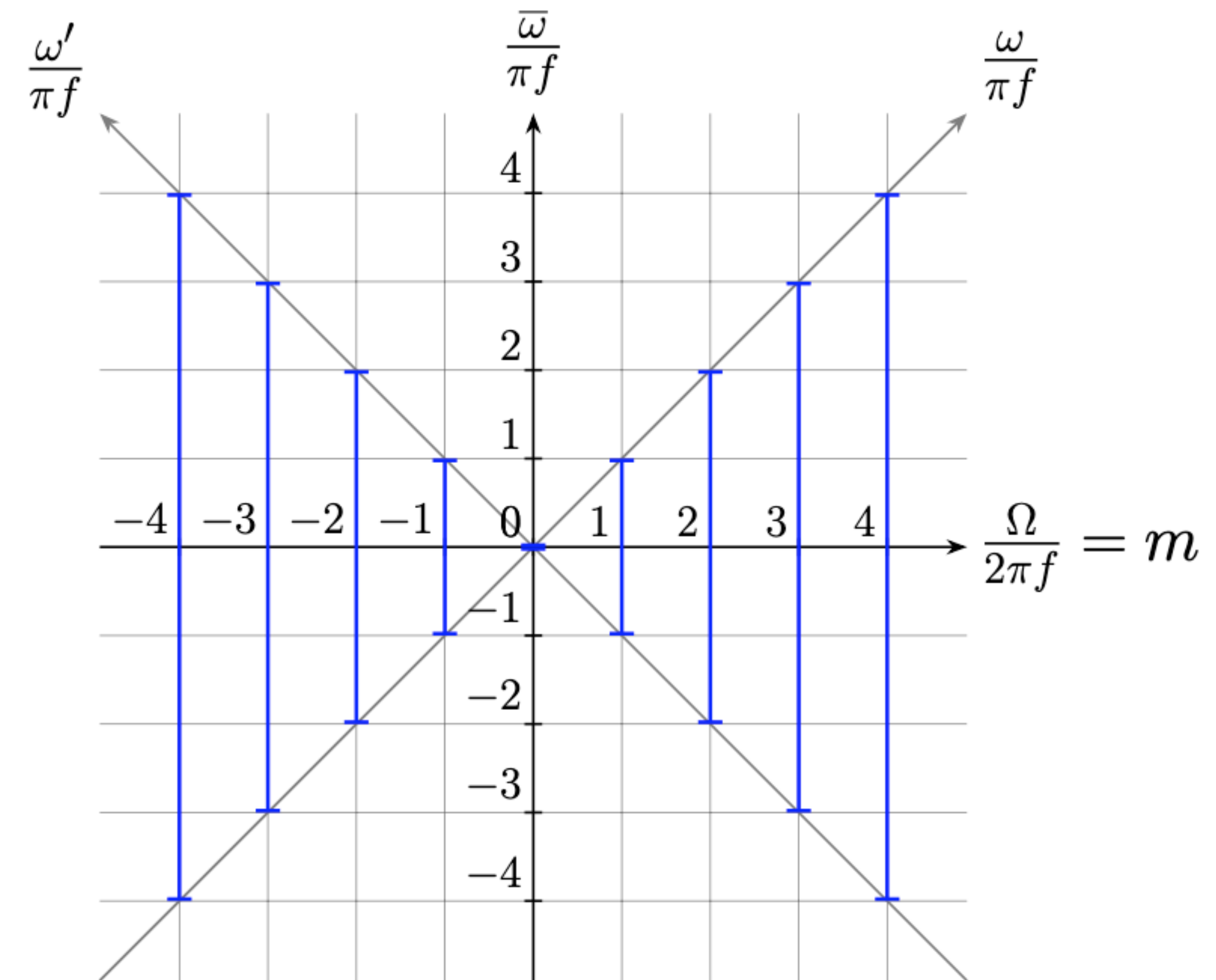
$$\widetilde{\mathcal{G}}_{\hat{\rho}}^{(e)}(\omega_A, \omega_B) \leftarrow \widetilde{\mathcal{G}}_{\hat{\rho}}^{(e)}\left(\bar{\omega} + \frac{\Omega}{2}, \bar{\omega} - \frac{\Omega}{2}\right)$$



Voltage pulse-train tomography

Efficient probing of the coherence space

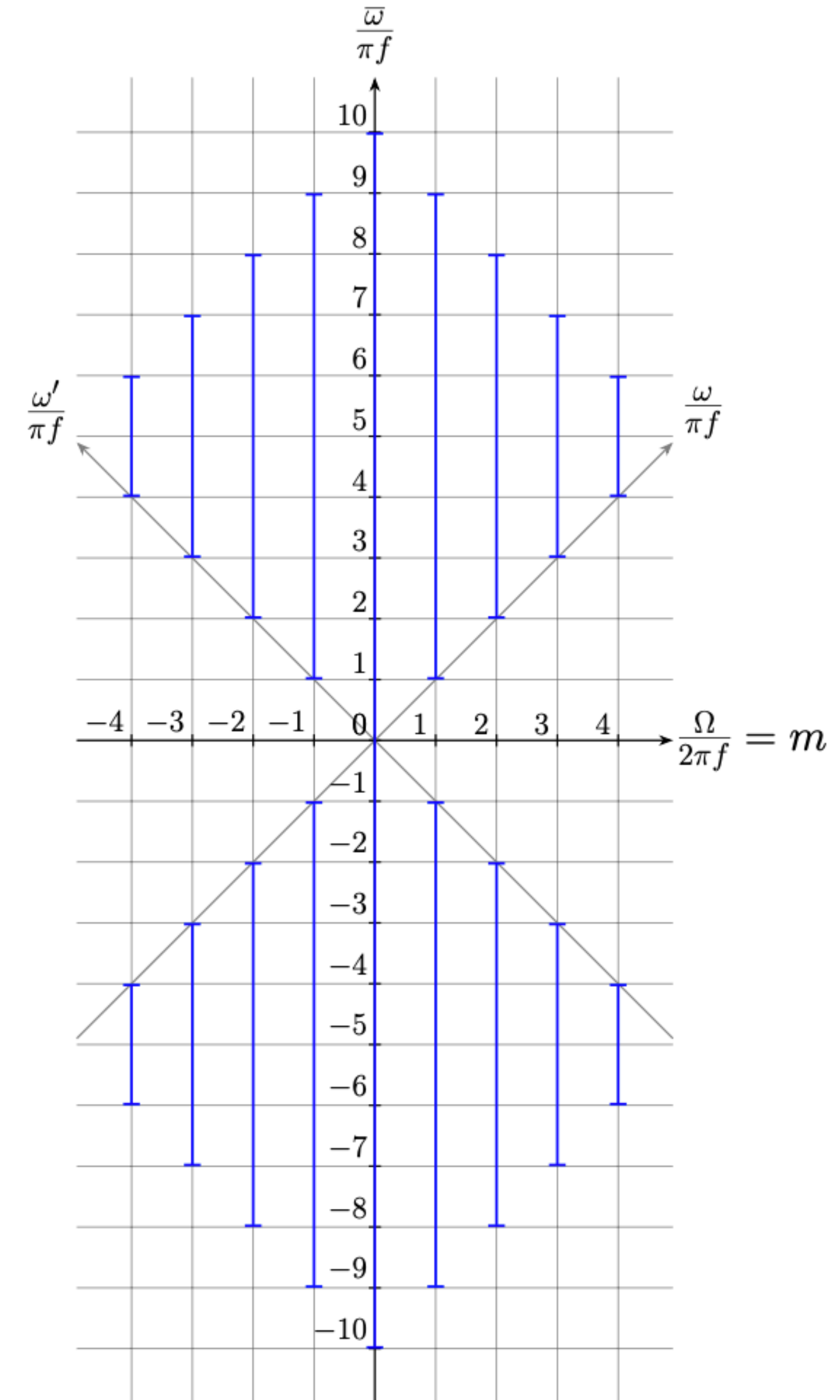
- **1st-order** $\mathcal{G}^{(e)}$ approximation in q_P
 - Access to the **electron-hole** coherences
 - Probe energy bands **centered on zero**
 - **Higher** harmonic \implies **wider** energy band
 - Vertical **translation** by adding a **bias voltage** V_{DC}
- **Adjust the probed areas:** more efficient because **less measurement points**



Voltage pulse-trains' coherence

Electron and hole excitation content

- **2nd-order** $\mathcal{G}^{(e)}$ approximation in q_P
 - Probe complementary areas **in the coherence space**
 - Access to **electron-electron** and **hole-hole** coherences
- Determine the content in **electron and hole excitations**
 - **e-e and h-h processes**: only accessible at the **2nd-order** in q_p
 - Linked to the **occupation numbers**: content of the unknown signal in terms of **particle excitations**



III. Two-electron coherent scattering

Second-order coherence function

Frequency space representation

- Separation of the **4D frequency space** into **two 2D spaces**

- Two « **diagonal** » dimensions ($\bar{\omega}_A$ and $\bar{\omega}_B$): **classical** plane
- Two « **off-diagonal** » dimensions (Ω_A and Ω_B): **quantum** plane

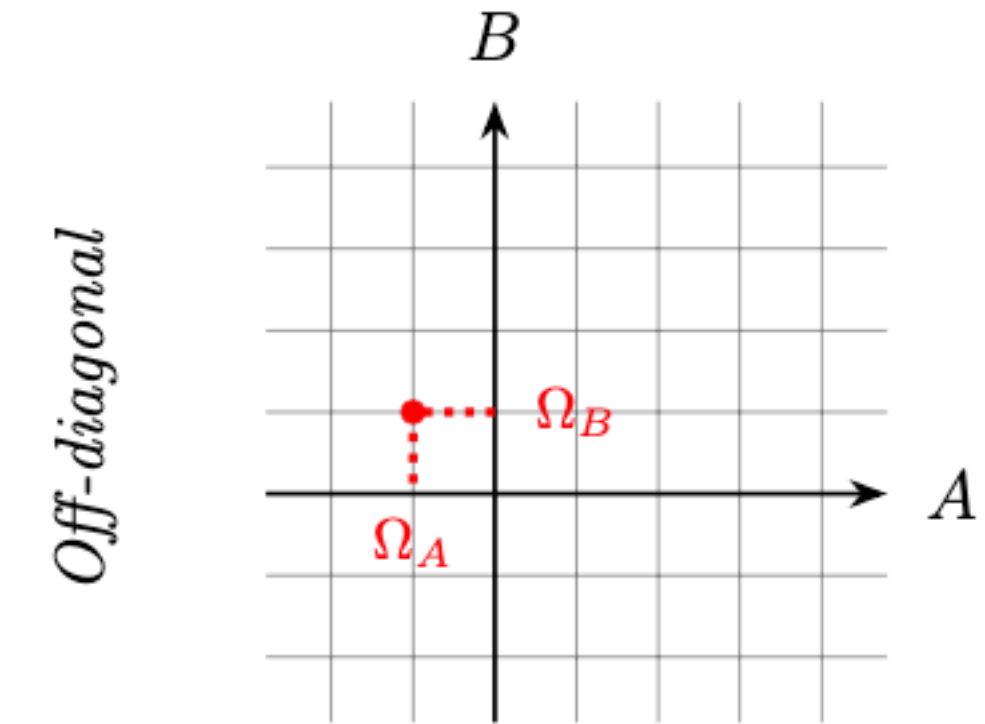
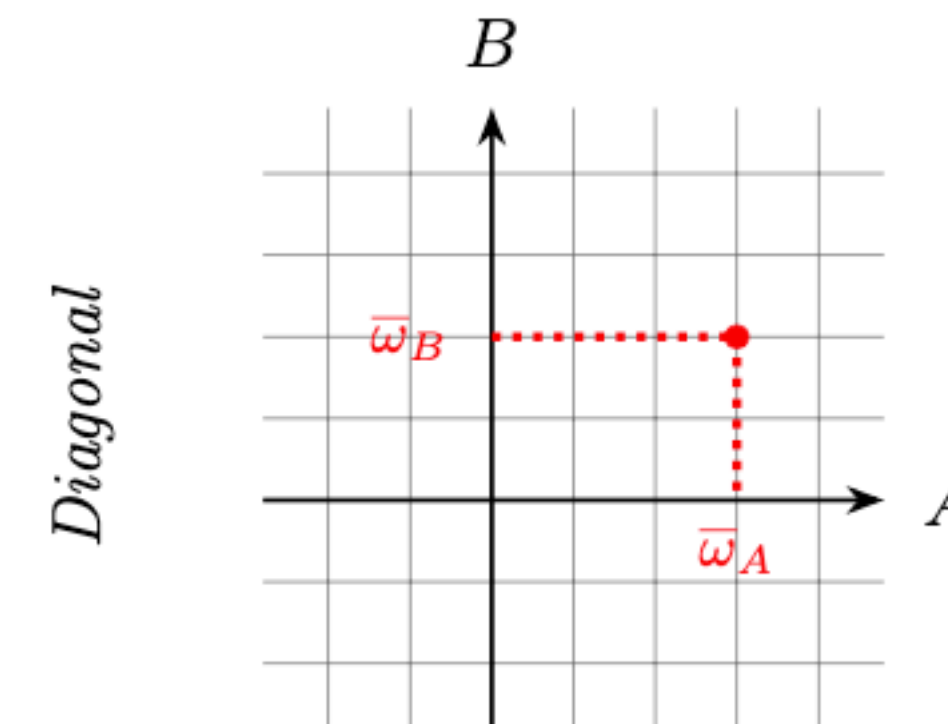
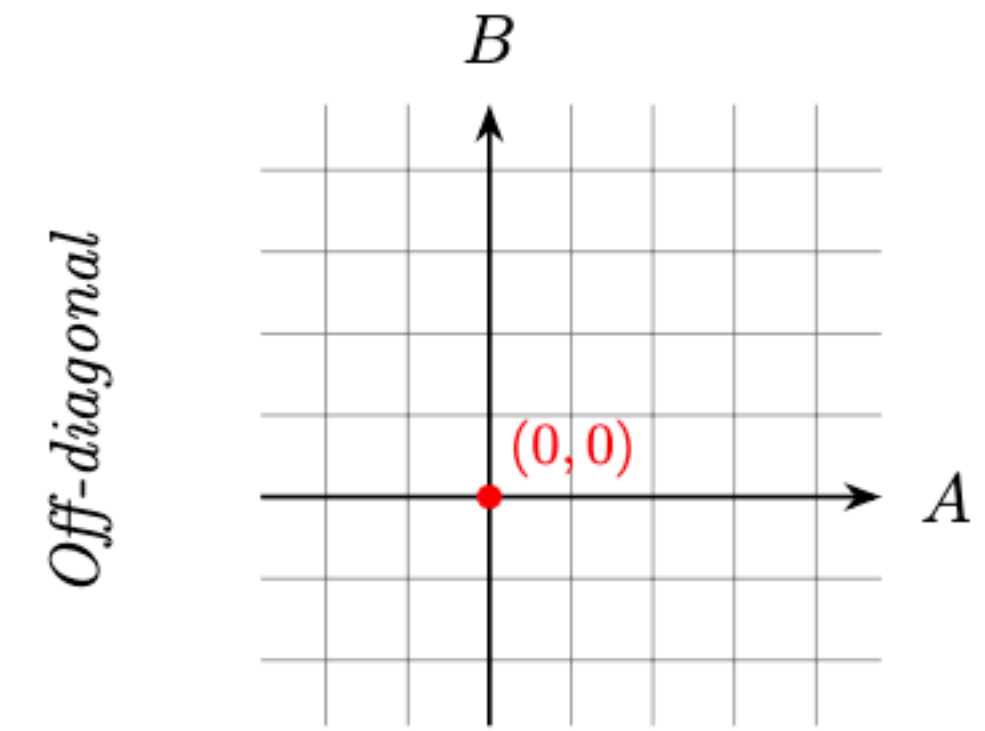
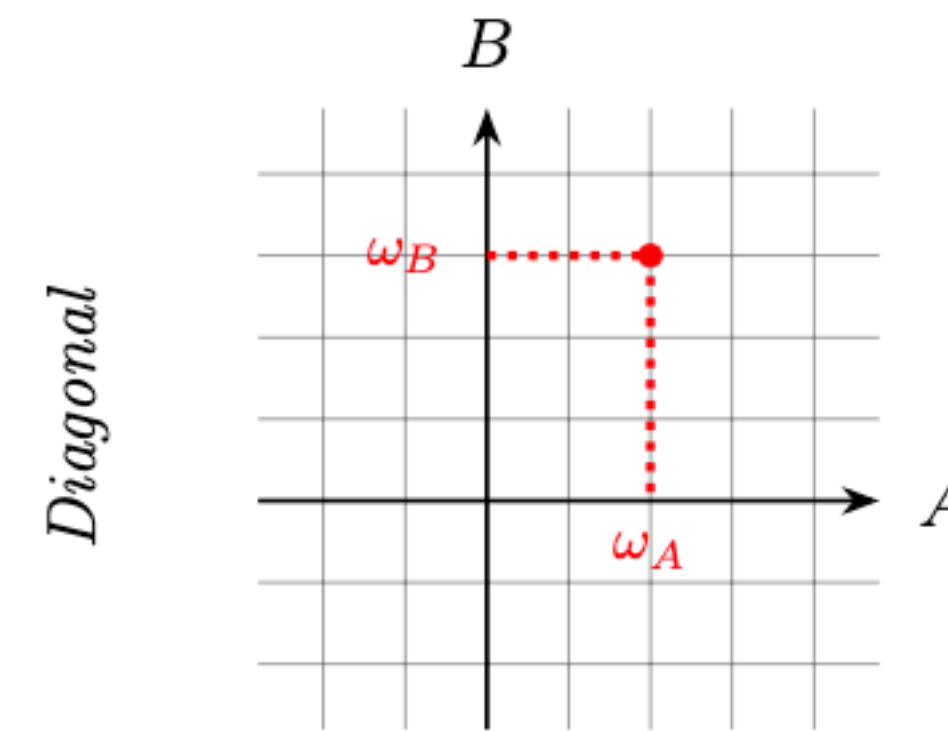
- **Diagonal** and **off-diagonal** variables: $\begin{cases} \bar{\omega}_A := \frac{\omega_A + \omega'_A}{2} \\ \Omega_A := \omega_A - \omega'_A \end{cases}$ and $\begin{cases} \bar{\omega}_B := \frac{\omega_B + \omega'_B}{2} \\ \Omega_B := \omega_B - \omega'_B \end{cases}$

$$\widetilde{\mathcal{G}}_{\hat{\rho}}^{(2e)}(\omega_A, \omega_B; \omega'_A, \omega'_B) = \widetilde{\mathcal{G}}_{\hat{\rho}}^{(2e)}\left(\bar{\omega}_A + \frac{\Omega_A}{2}, \bar{\omega}_B + \frac{\Omega_B}{2}; \bar{\omega}_A - \frac{\Omega_A}{2}, \bar{\omega}_B - \frac{\Omega_B}{2}\right)$$

From 4D to (2+2)D in the frequency space

Simple examples

- **Plane waves** at energies ω_A and ω_B
 - $|\psi\rangle = \hat{c}_A^\dagger[\omega_A] \hat{c}_B^\dagger[\omega_B] |F\rangle$ with $|F\rangle := |F\rangle_A \wedge |F\rangle_B$
 - Perfectly localized \implies purely **classical**
- Superposition of **two Slater determinants**
 - $|\psi\rangle = \frac{1}{\sqrt{2}} \left(\hat{c}_A^\dagger[\omega_A] \hat{c}_B^\dagger[\omega_B] + \hat{c}_A^\dagger[\omega'_A] \hat{c}_B^\dagger[\omega'_B] \right) |F\rangle$
 - States **superposition** \implies **off-diagonal** terms



Cauchy-Schwarz entanglement witness

Expression in the frequency domain

- Cauchy-Schwarz « full- $\mathcal{G}^{(2e)}$ » **entanglement witness**

$$\langle \hat{A}_1 \hat{A}_2 \hat{B}_1 \hat{B}_2 \rangle_{\hat{\rho}}^2 \leq \langle \hat{A}_1 \hat{A}_1^\dagger \hat{B}_2^\dagger \hat{B}_2 \rangle_{\hat{\rho}} \langle \hat{A}_2^\dagger \hat{A}_2 \hat{B}_1 \hat{B}_1^\dagger \rangle_{\hat{\rho}}$$

- **Sufficient (but not necessary)** condition to detect **entangled states**

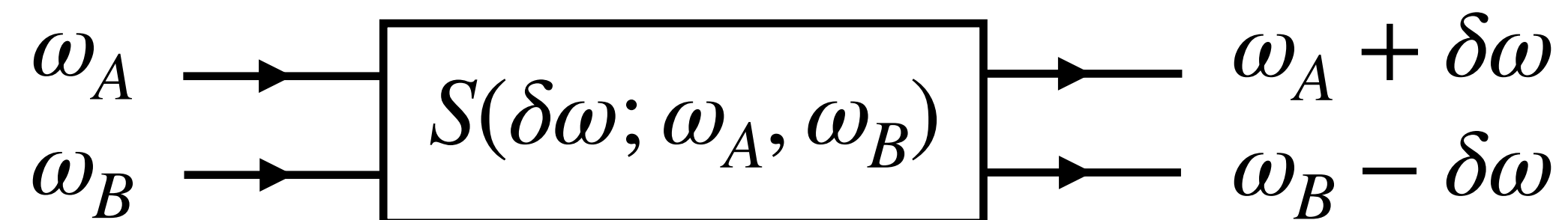
- **Separable** state: $|\psi\rangle = \hat{O}_A \hat{O}_B |F\rangle$ (with $\hat{O}_{A/B}$ **creation operators** acting on states of $\mathcal{H}_{A/B}$)

$$|\widetilde{\mathcal{G}}_{\hat{\rho}}^{(2e)}(\omega_A, \omega_B; \omega'_A, \omega'_B)|^2 \leq \widetilde{\mathcal{G}}_{\hat{\rho}}^{(2e)}(\omega_A, \omega'_B; \omega_A, \omega'_B) \widetilde{\mathcal{G}}_{\hat{\rho}}^{(2e)}(\omega'_A, \omega_B; \omega'_A, \omega_B)$$

Two-electron coherent scattering model

Scattering model for « high energy » electrons

- Two **electrons** propagate along **two channels** A and B with energies (ω_A, ω_B)
- **Scattering process** described by a **scattering matrix** \hat{S}
 - Limited bandwidth for the **exchanged** energy: $\delta\omega \in [-\omega_A, \omega_B]$
 - **Unitary** matrix \hat{S} , function of ω_A , ω_B , and $\delta\omega$
- **Coherent** scattering with **conservation** of the total energy: $E_{tot} = \omega_A + \omega_B$



Collision of energy-localized wave-packets

The outgoing two-electron state

- Incoming electrons: **perfectly localized in energy** (at ω_A and ω_B)

$$|\psi\rangle_{in} := \hat{c}_A^\dagger[\omega_A] \hat{c}_B^\dagger[\omega_B] |F\rangle \quad \text{with} \quad |F\rangle := |F\rangle_A \wedge |F\rangle_B$$

- **Scattered** electrons: superposition of **all the possible energy transfers**

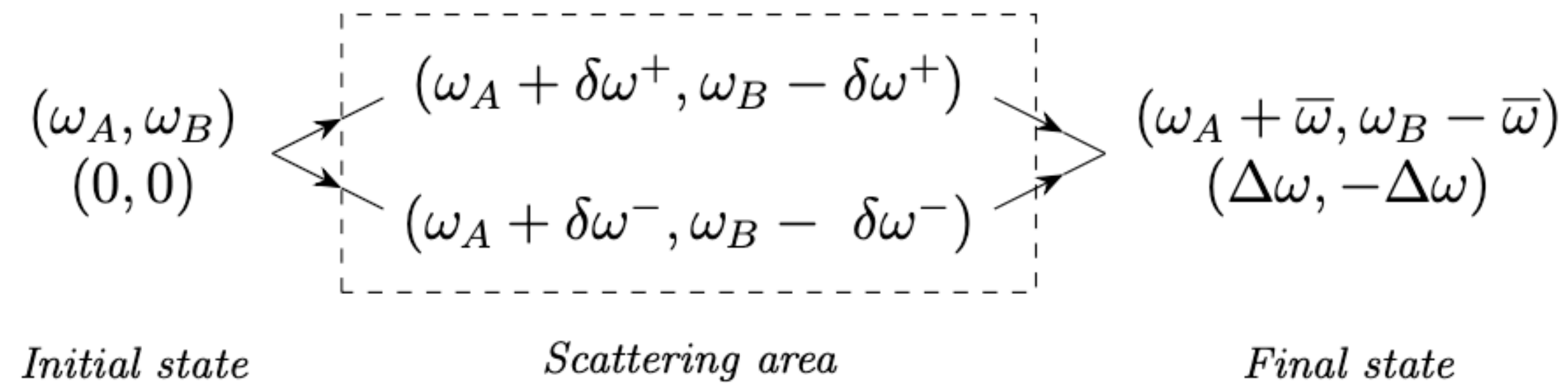
$$|\psi\rangle_{out} := \int_{\mathbb{R}} d(\delta\omega) S(\delta\omega; \omega_A, \omega_B) \hat{c}_A^\dagger[\omega_A + \delta\omega] \hat{c}_B^\dagger[\omega_B - \delta\omega] |F\rangle$$

- **Goal of the study:** apply the full- $\mathcal{G}^{(2e)}$ criterion with $\hat{\rho}_{out} := |\psi\rangle_{out} \langle\psi|_{out}$

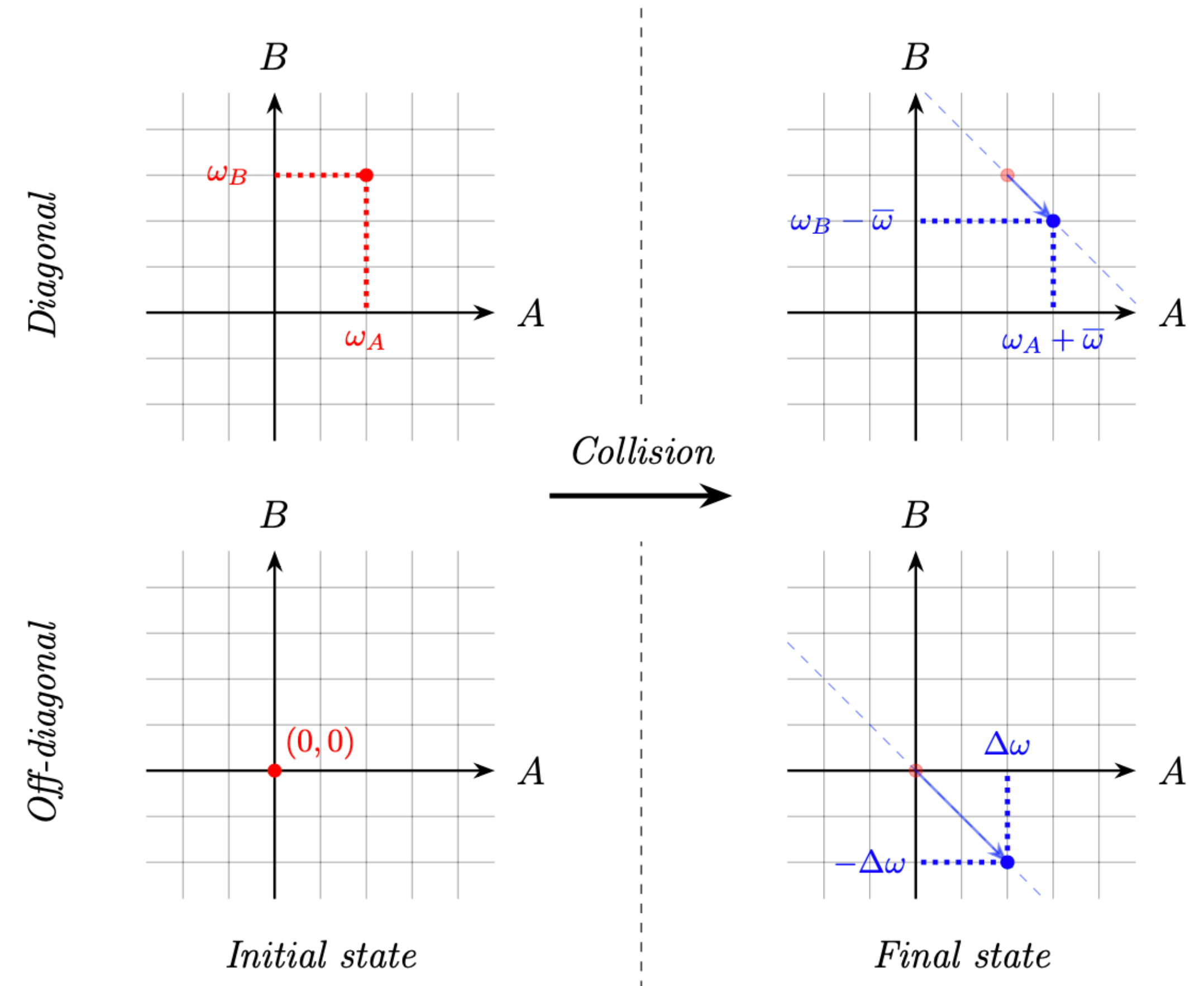
Visualization of the scattering process

Effect on the two-electron coherence

- Considering **two quantum paths**



- $\bar{\omega} := \frac{\delta\omega^+ + \delta\omega^-}{2}$ and $\Delta\omega := \delta\omega^+ - \delta\omega^-$
- Conserved** quantities: $\omega_A + \omega_B$ and $\Omega_A + \Omega_B$

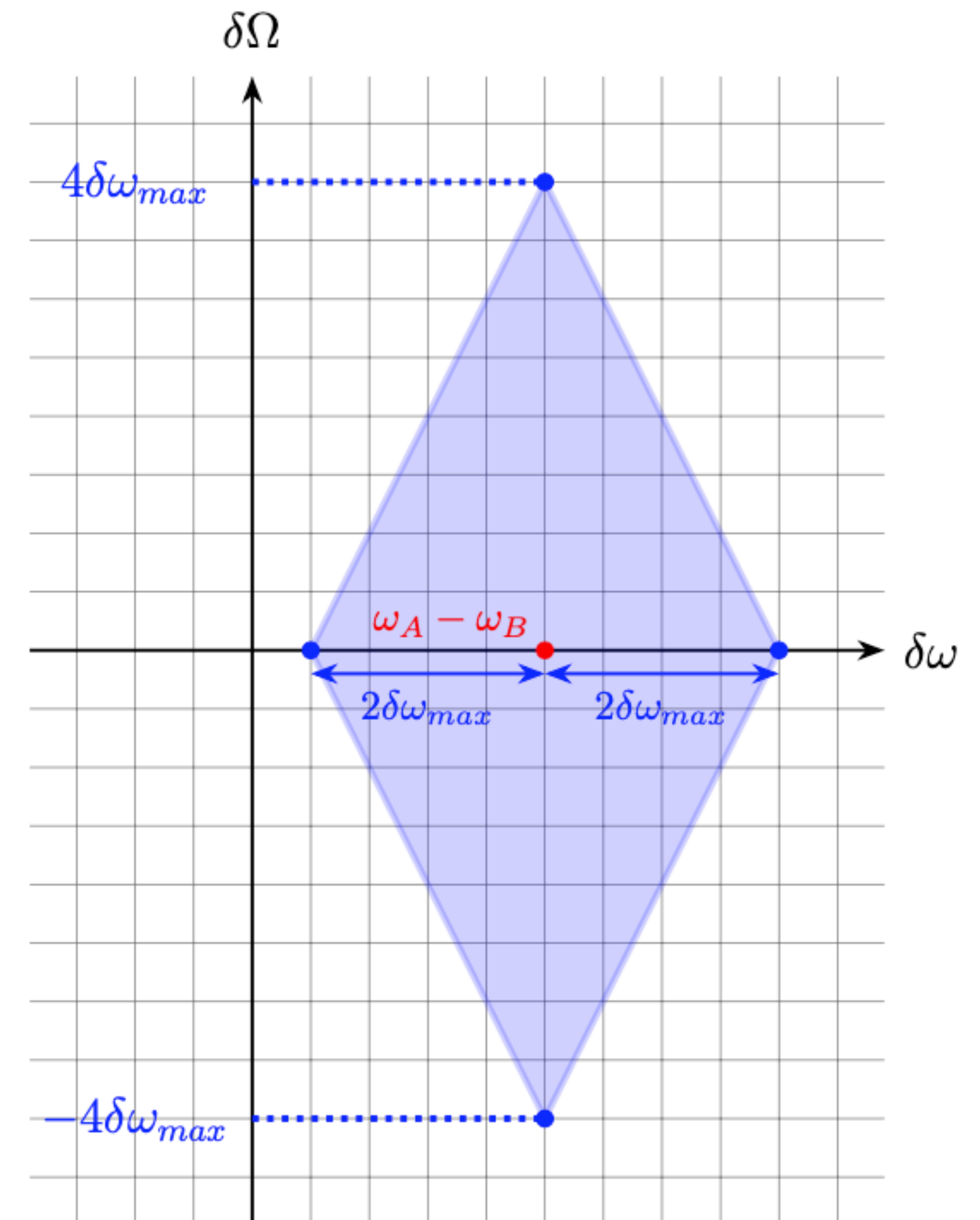


Representation of the scattered states

Two-dimensional visualization

- View in the plane $(\delta\omega, \delta\Omega) := (\omega_A - \omega_B, \Omega_A - \Omega_B)$
- Detection of both electrons **above the Fermi sea**
 - $|\delta\omega^\pm| \leq \delta\omega_{max}$: **rectangle** in the $(\delta\omega^+, \delta\omega^-)$ plane
- **Rotation** and **rescaling** with $(\bar{\omega}, \Delta\omega)$

Scattered states represent a **diamond** in the $(\delta\omega, \delta\Omega)$ plane



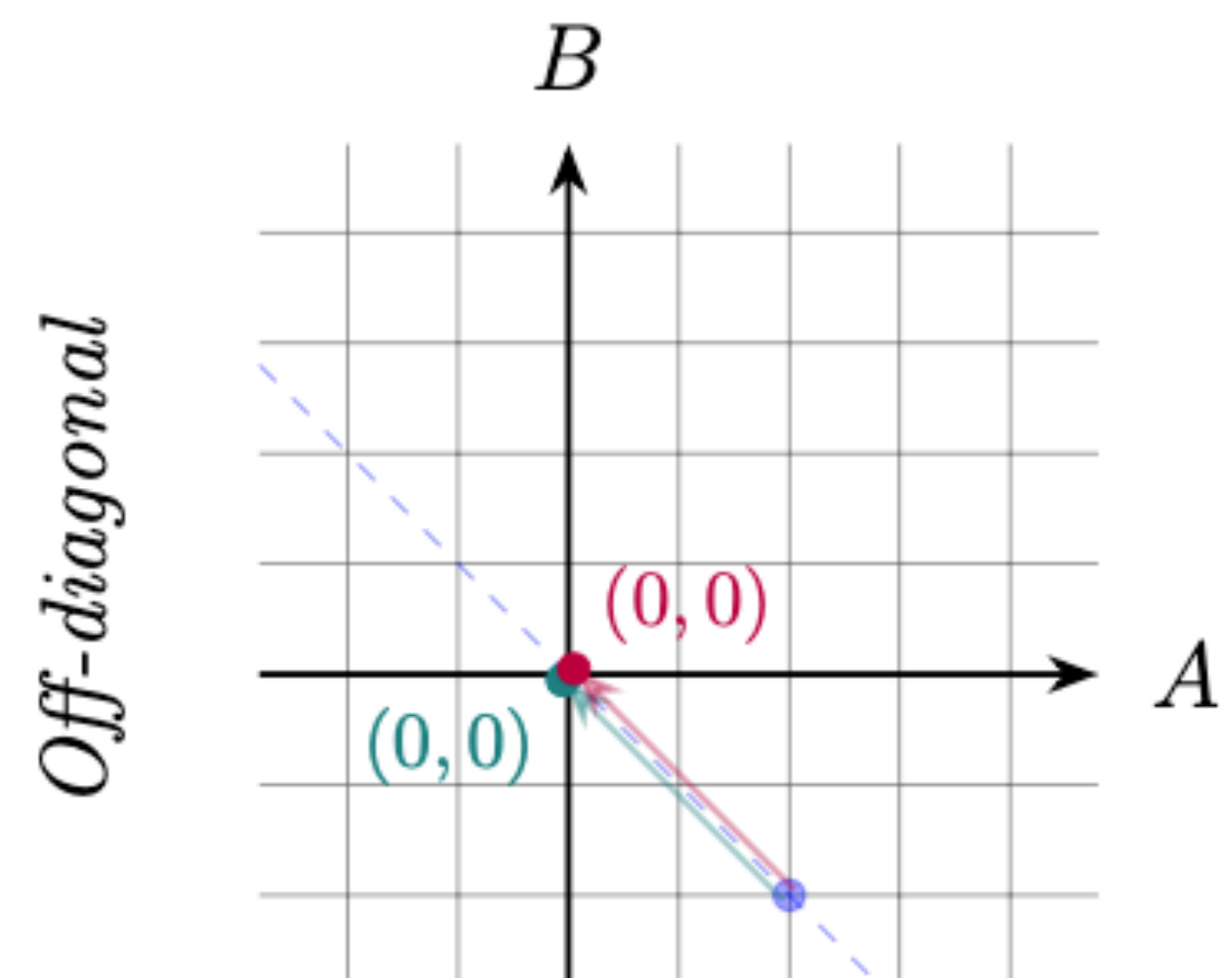
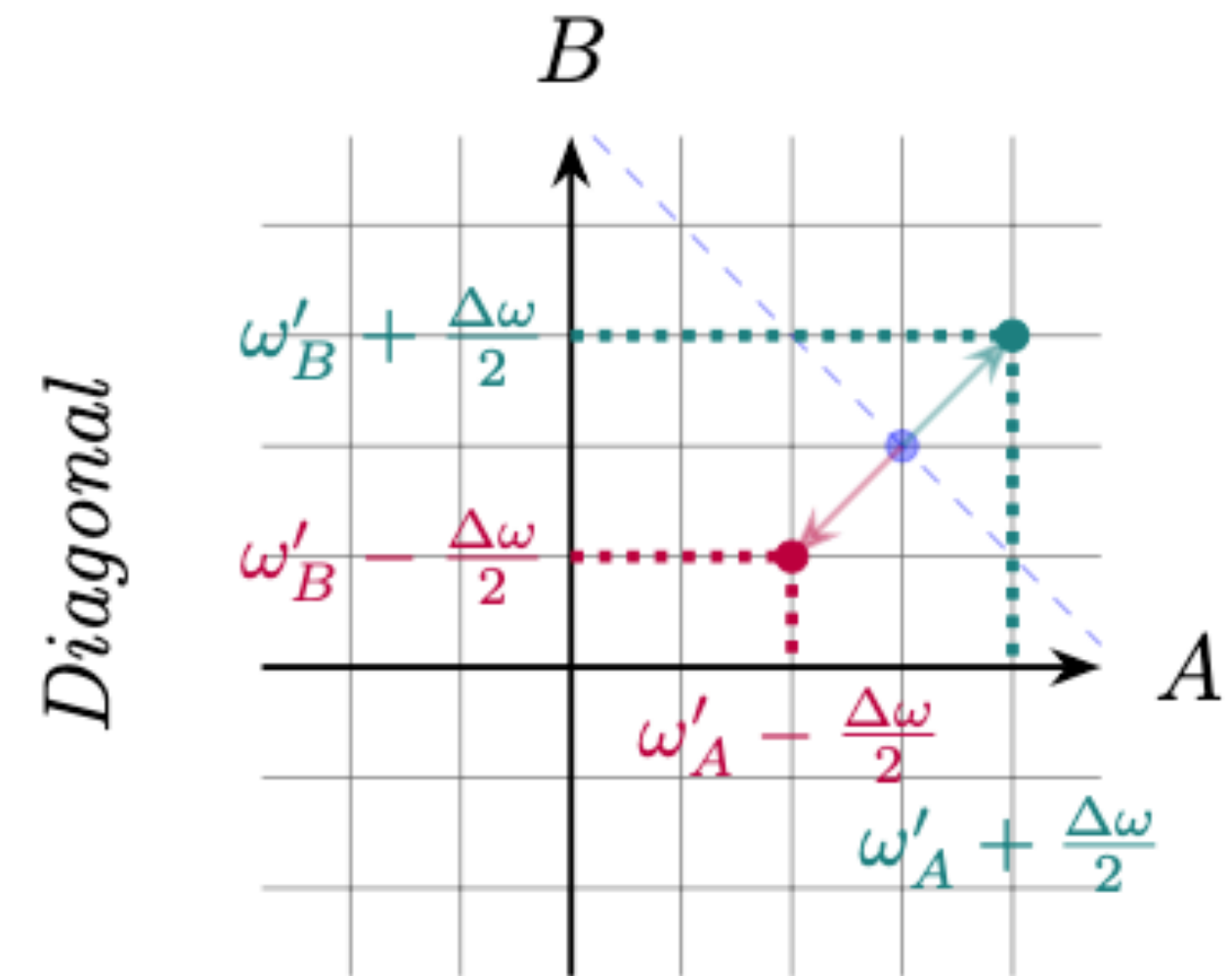
Cauchy-Schwarz entanglement witness

Four-dimensional visualization

$$|\widetilde{\mathcal{G}}_{\hat{\rho}}^{(2e)}(\omega_A, \omega_B; \omega'_A, \omega'_B)|^2 \leq \widetilde{\mathcal{G}}_{\hat{\rho}}^{(2e)}(\omega_A, \omega'_B; \omega_A, \omega'_B) \widetilde{\mathcal{G}}_{\hat{\rho}}^{(2e)}(\omega'_A, \omega_B; \omega'_A, \omega_B)$$

- Coordinates of the **right-hand side** points
 - **Diagonal** component: **out of the energy conservation** line
 - **No off-diagonal** component: C.S. points are **always diagonal**
- **Witness violated** as soon as $\Delta\omega \neq 0$ ($\iff \delta\omega^+ \neq \delta\omega^-$)

The scattering process always creates entanglement



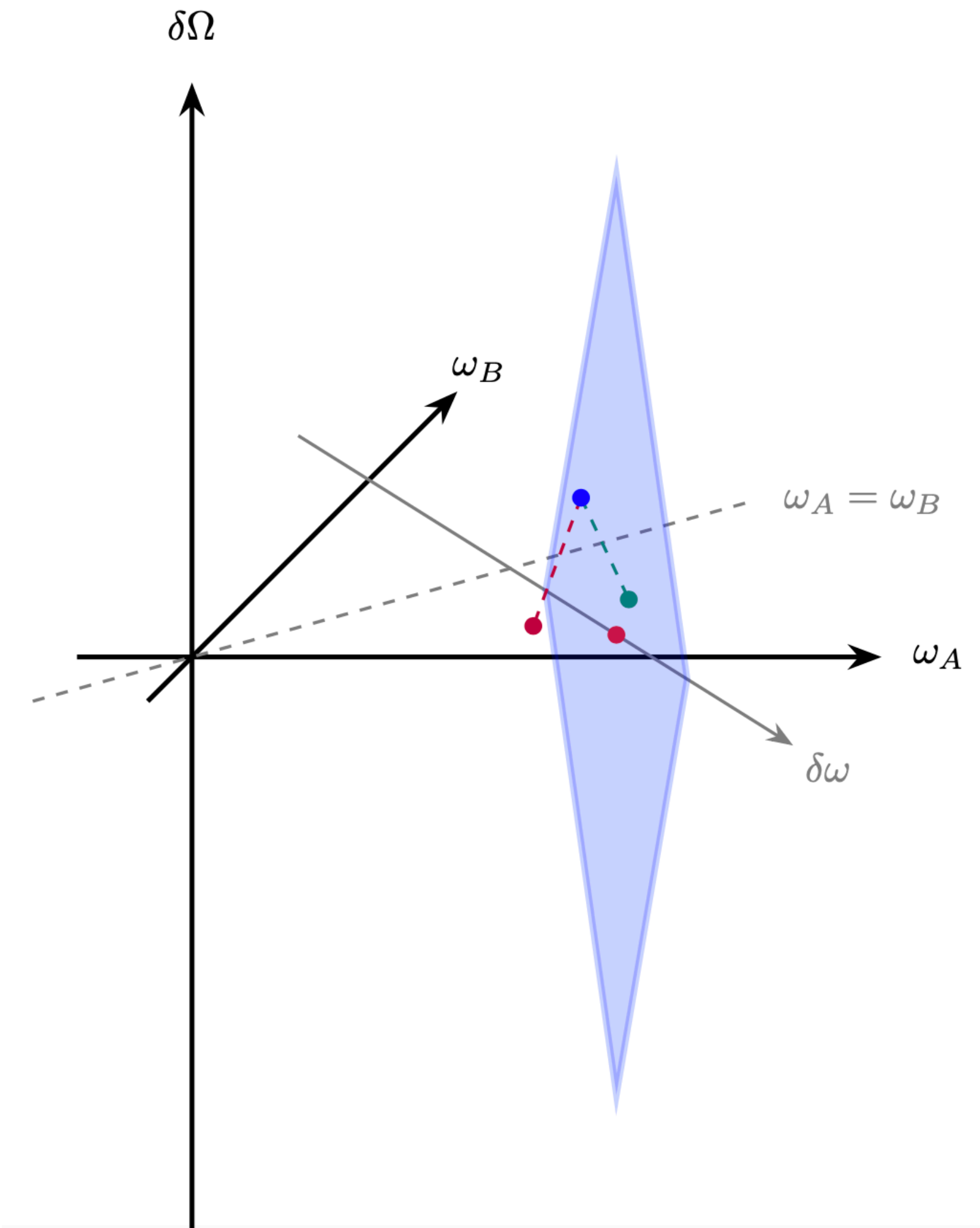
Collision-induced entanglement

Take-home messages

- Scattered states: « **flat** » **diamond** in the $(\delta\omega, \delta\Omega)$ plane
- **Expression in terms of \hat{S} matrix coefficients:**

$$|S(\delta\omega^+; \omega_A, \omega_B) S(\delta\omega^-; \omega_A, \omega_B)^*|^2 \leq 0$$

- **Scattering \implies C.S. points out of the diamond**
- **Diamond's flatness** due to the **perfect localization in energy** of the incoming electrons



Conclusion and perspectives

Conclusion and perspectives

- **Improvement of the HOM tomography protocol: important gain of time**
 - Tune the **harmonics** and the **bias voltage** to probe the coherence more efficiently
 - Excitation content of low voltage pulses (work in progress)
- **Creation of entanglement** in a two-particle **coherent** scattering model
 - Study **more realistic wave-packets** : Landau wave-packets, Levitons
 - Specifying the **scattering model**: explicit expression of the \hat{S} matrix
 - **Incoherent scattering**: exchange of energy **with the environment**
- **Perspective**: one and two electron tomography by **photo-assisted filtering**

**Thank you for
your attention!**



Appendices

A. Parity super-selection rule

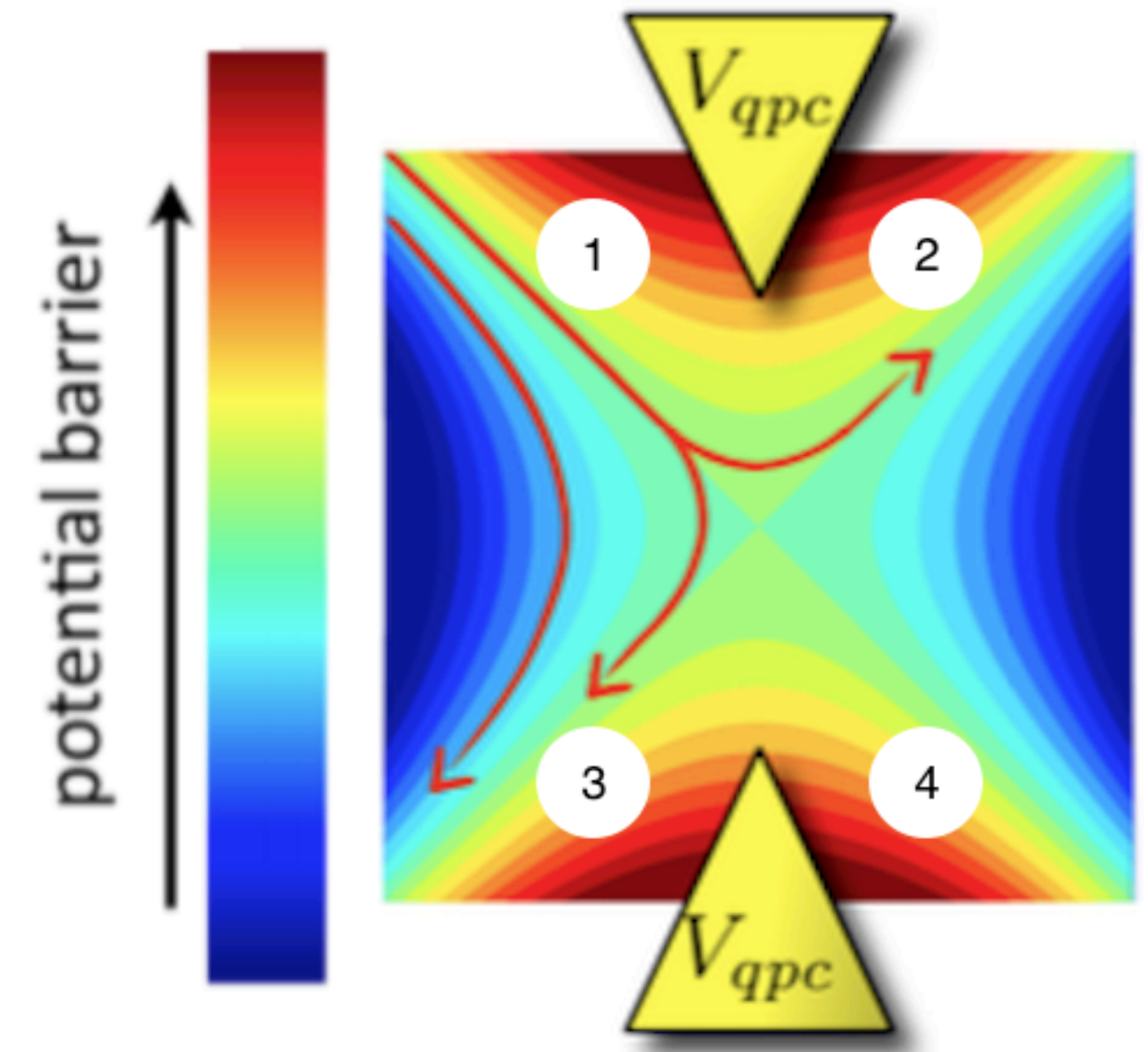
Appendices

- **Any superposition of fermionic states with different number-of-particle parities is forbidden**
- Comes from **Einstein's causality principle**: without SSR, **no-signaling is violated**
 - Consequence: **no fermionic qubit with 1 mode**, as $|\psi\rangle = \alpha |0\rangle + \beta |1\rangle$ is forbidden
 - **Limitation of the superposition principle** (fundamental principle of QM) for fermions
- Basis for the development of a **fermionic quantum theory of information**

B. Quantum point contact

Appendices

- Fermionic **beam splitter**: **delocalizes** an electron into **two channels**
- Two **electrodes** in a **2D electron gas**
 - Application of a **potential** V_{qpc} to both electrodes
 - **Coulomb repulsion** creates an **energetic barrier**
 - A fraction of the electron **tunnels** through the QPC
- The **higher** V_{qpc} , the **lower fraction** exits the QPC

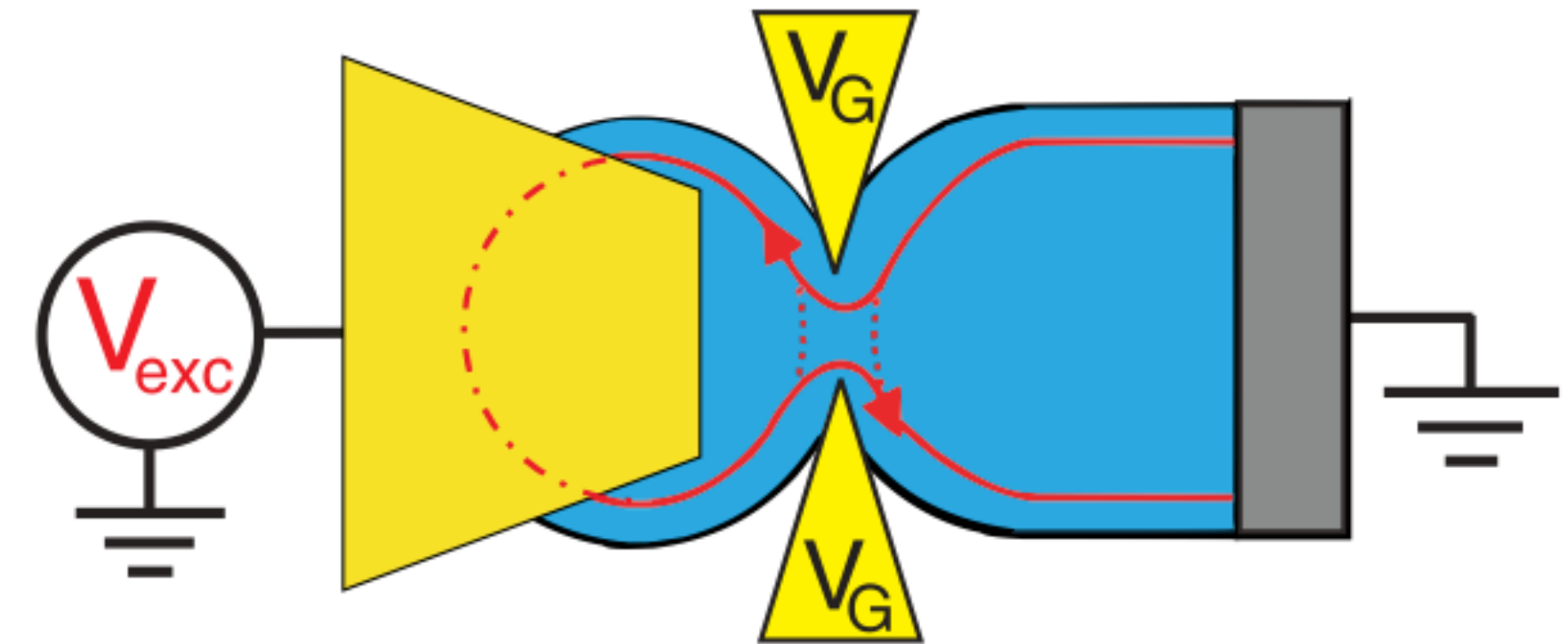


Bocquillon et al., Phys. Rev. Lett. 108 (2012), 196803.

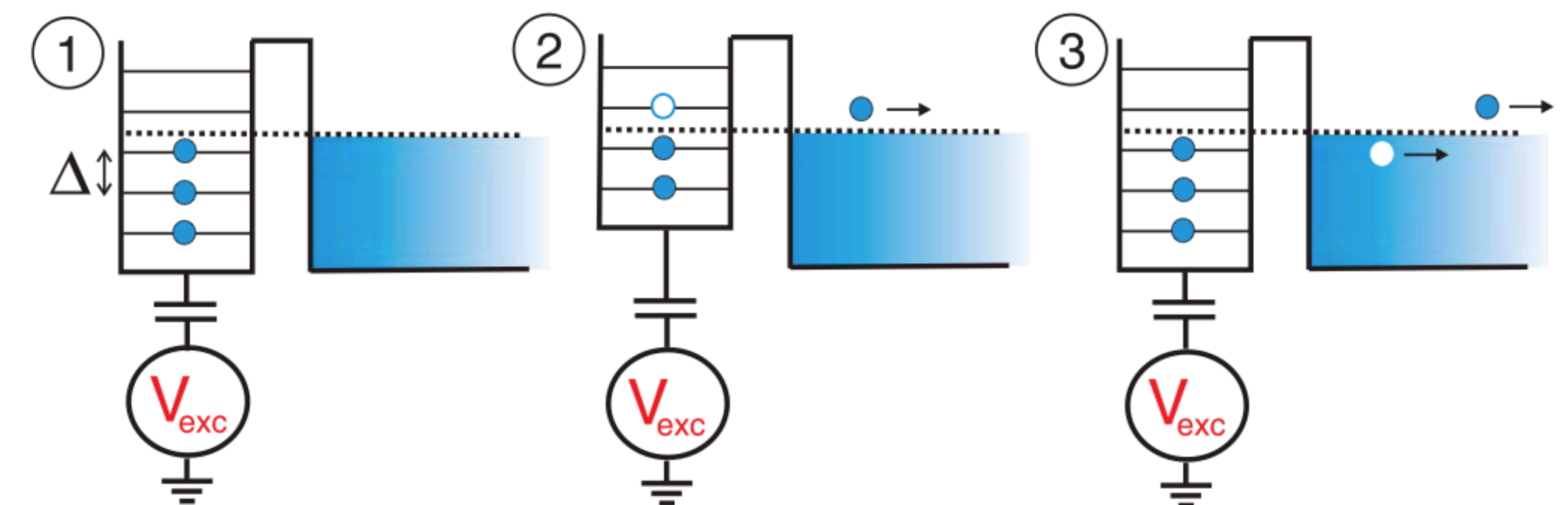
C. Mesoscopic capacitor

Appendices

- **On-demand** source of **single** electronic excitations
- **QPC** separating a 2DEG into two areas
 - **Reservoir** with **constant potential**
 - Area submitted to a **varying potential** V_{exc}
- **Periodic** emission of an **electron** and a **hole** excitations



Fève, Thèse de doctorat, Université Pierre et Marie Curie - Paris VI, Nov. 2006.



Filippone et al., Entropy 22, 8 (July 2020), 847.

D. Cauchy-Schwarz inequalities

Appendices

- General Cauchy-Schwarz **inequality** (second-order coherence):

$$|\widetilde{\mathcal{G}}_{\hat{\rho}}^{(2e)}(\omega_A, \omega_B; \omega'_A, \omega'_B)|^2 \leq \widetilde{\mathcal{G}}_{\hat{\rho}}^{(2e)}(\omega_A, \omega_B; \omega_A, \omega_B) \widetilde{\mathcal{G}}_{\hat{\rho}}^{(2e)}(\omega'_A, \omega'_B; \omega'_A, \omega'_B)$$

- Cauchy-Schwarz **witnesses** (Hillery-Zubairy):

$$|\widetilde{\mathcal{G}}_{\hat{\rho}}^{(2e)}(\omega_A, \omega_B; \omega'_A, \omega'_B)|^2 \leq \widetilde{\mathcal{G}}_{\hat{\rho}}^{(2e)}(\omega_A, \omega'_B; \omega_A, \omega'_B) \widetilde{\mathcal{G}}_{\hat{\rho}}^{(2e)}(\omega'_A, \omega_B; \omega'_A, \omega_B) \quad (\text{full } \mathcal{G}^{(2e)}\text{-criterion})$$

$$|\mathcal{G}^{(e)}(\omega_A, \omega_B)|^2 \leq \mathcal{G}^{(2e)}(\omega_A, \omega_B; \omega_A, \omega_B) \quad (\text{hybrid criterion})$$

$$|\mathcal{G}^{(e)}(\omega_A, \omega_B)|^2 \leq (1 - \mathcal{G}^{(e)}(\omega_A; \omega_A)) \mathcal{G}^{(e)}(\omega_B; \omega_B) \quad (\text{full } \mathcal{G}^{(e)}\text{-criterion})$$

E. Spin-operator representation

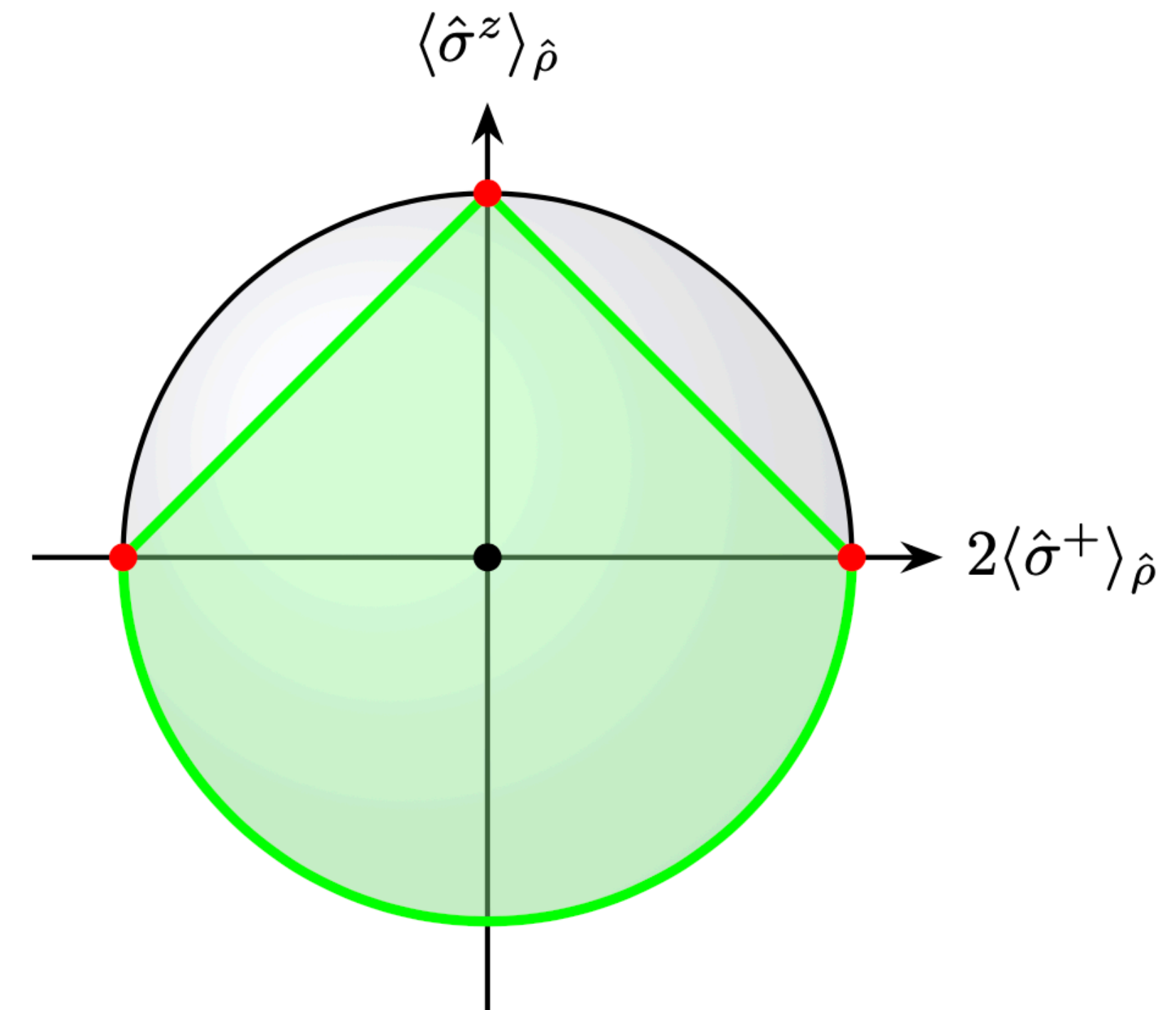
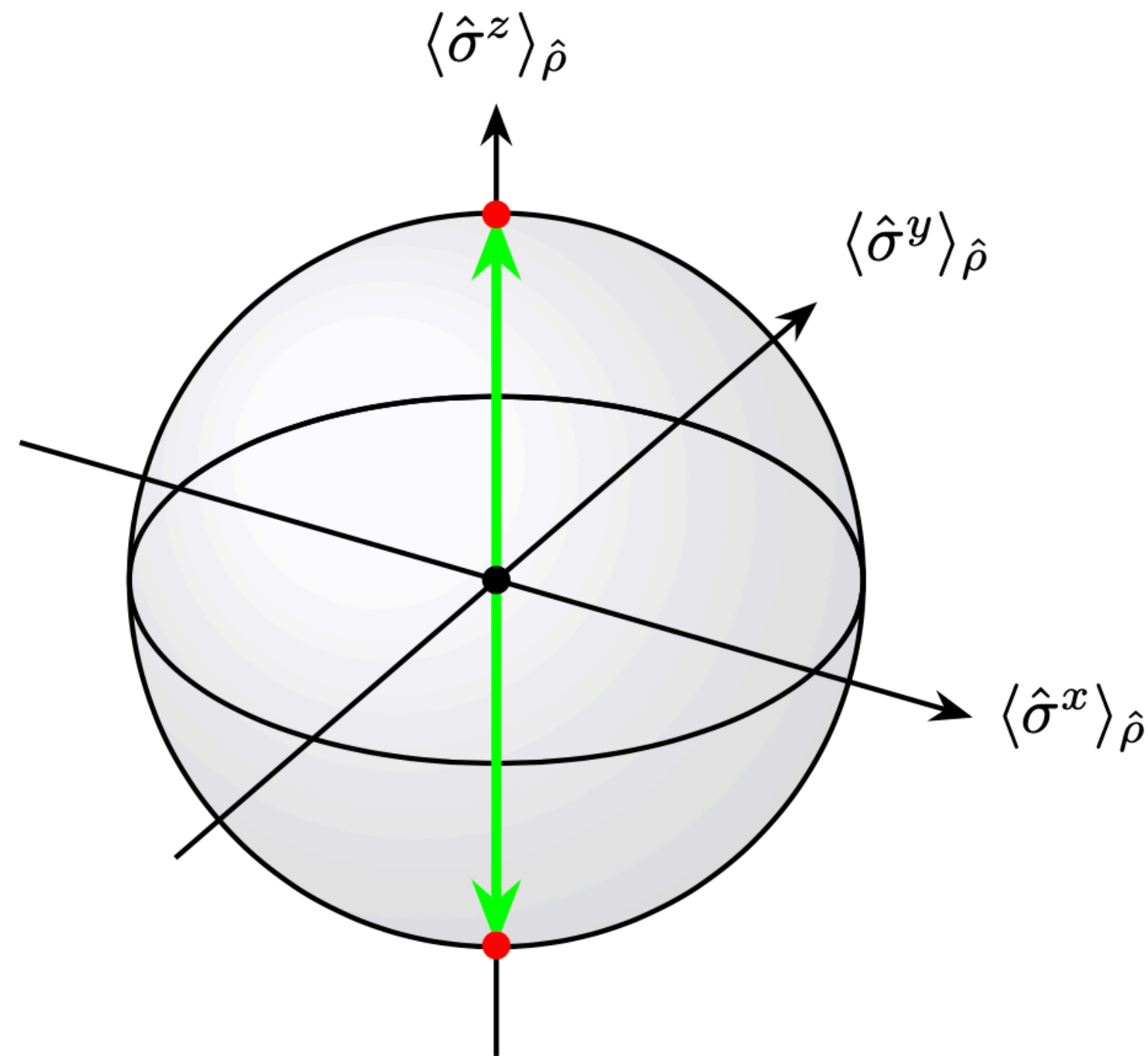
Appendices

- $$\begin{cases} \hat{\sigma}^x = \hat{\psi}_A^\dagger[\varphi] \hat{\psi}_B[\varphi'] + \hat{\psi}_B^\dagger[\varphi'] \hat{\psi}_A[\varphi] \\ \hat{\sigma}^y = i(\hat{\psi}_B^\dagger[\varphi'] \hat{\psi}_A[\varphi] - \hat{\psi}_A^\dagger[\varphi] \hat{\psi}_B[\varphi']) \text{ and } \\ \hat{\sigma}^z = \hat{\psi}_A^\dagger[\varphi] \hat{\psi}_A[\varphi] - \hat{\psi}_B^\dagger[\varphi'] \hat{\psi}_B[\varphi'] \end{cases} \quad \begin{cases} \hat{\sigma}^+ = \frac{1}{2}(\hat{\sigma}^x + i\hat{\sigma}^y) = \hat{\psi}_A^\dagger[\varphi] \hat{\psi}_B[\varphi'] \\ \hat{\sigma}^- = \frac{1}{2}(\hat{\sigma}^x - i\hat{\sigma}^y) = \hat{\psi}_B^\dagger[\varphi'] \hat{\psi}_A[\varphi] \\ \hat{1}^\sigma = \hat{\psi}_A^\dagger[\varphi] \hat{\psi}_A[\varphi] + \hat{\psi}_B^\dagger[\varphi'] \hat{\psi}_B[\varphi'] \end{cases}$$
- Satisfy the **Fermi algebra** $\{\hat{\sigma}^\alpha, \hat{\sigma}^\beta\} = 2i\varepsilon_{\alpha\beta\gamma}\hat{\sigma}^\gamma$
- **Hybrid** criterion: $\langle \hat{\sigma}^+ \rangle_{\hat{\rho}} = 0$ **Full** $\mathcal{G}^{(e)}$ -criterion: $2|\langle \hat{\sigma}^+ \rangle_{\hat{\rho}}| \leq 1 - \langle \hat{\sigma}^z \rangle_{\hat{\rho}}$

E. Spin-operator representation

Appendices

- Hybrid witness: $\langle \hat{\sigma}^+ \rangle_{\hat{\rho}} = 0$
- Full- $\mathcal{G}^{(e)}$ witness: $2|\langle \hat{\sigma}^+ \rangle_{\hat{\rho}}| \leq 1 - \langle \hat{\sigma}^z \rangle_{\hat{\rho}}$



F. Collision of two Landau wave-packets

Appendices

- **Spreading** of the wave-packet
- The diamond is « **spread** » in the $\omega_A = \omega_B$ direction
- Witness **respected**: **overlap** between the scattered state and the C.S. points

